Expression and Spectroscopic Analysis of Soluble Nicotinic Acetylcholine Receptor Fragments Derived from the Extracellular Domain of the α-Subunit†

Marianne A. Grant, Lisa N. Gentile,‡ Qing-Luo Shi, Maria Pellegrini, and Edward Hawrot*

Department of Molecular Pharmacology, Physiology, and Biotechnology, Division of Biology and Medicine, Brown University, Providence, Rhode Island 02912

Received December 22, 1998; Revised Manuscript Received May 10, 1999

ABSTRACT: To facilitate structural studies of the ligand binding region from the nicotinic acetylcholine receptor (nAChR), we have developed methods for the high-level expression and purification of an important functional portion of the N-terminal extracellular domain (ECD) of the α-subunit. Two soluble receptor fragments comprising residues 143−210 of the *Torpedo californica* α-subunit were expressed in *E. coli*: αT68His$_6$, which contains a histidine tag, and αT68M1, which includes the first transmembrane region, M1, of the α-subunit. Both proteins demonstrate saturable, high-affinity α-bungarotoxin (Bgtx) binding with an apparent equilibrium K_D (3 nM) that is comparable to the affinities reported for preparations comprising the entire α-subunit ECD. These results demonstrate that the ECD determinants required for Bgtx recognition of the α-subunit are entirely specified by residues 143−210. The binding of small ligands was demonstrated in competition assays with ^{125}I-Bgtx yielding K_I values of 58 and 105 μM for *d*-tubocurarine and nicotine, respectively. Circular dichroism (CD) analysis of monomeric αT68His$_6$ protein revealed considerable secondary structure. Furthermore, a cooperative, two-state folding transition was observed upon urea denaturation. To circumvent concentration-dependent aggregation of the αT68His$_6$ protein at the millimolar concentrations needed for NMR study, we utilized the M1 transmembrane domain to anchor the recombinant receptor fragment onto membrane-mimicking micelles. Monodispersed preparations of αT68M1 in dodecylphosphocholine micelles demonstrate high-affinity Bgtx binding and considerable secondary structure by CD. The structural features revealed in the CD profile appear to undergo a cooperative, two-state folding transition upon thermal denaturation. Initial NMR studies suggest that micellar preparations of the αT68M1 fragment are amenable to further high-resolution heteronuclear NMR analysis.

Nicotinic acetylcholine receptors (nAChRs)[1] comprise a family of integral-membrane ion channels that bind two molecules of acetylcholine (ACh) to mediate synaptic transmission in the nervous system. They are the best characterized members of a superfamily of highly homologous ligand-gated ion channels that includes the glycine, γ-aminobutyric acid$_A$, and 5-HT$_3$ receptors (*1*). The muscle-type nAChR at the neuromuscular junction and at the related synapse in the electric organ of *Torpedo* consists of a pentameric complex of four homologous subunits (β-, δ-, γ-, and two α-subunits) surrounding a cation-selective channel (*2*). The N-terminal half of each subunit, ∼210−230 residues, is extracellular and is followed by the first of four putative transmembrane-spanning domains (M1−M4). The high homology among ligand-gated ion channels suggests that atomic resolution structural studies of the nAChR will elucidate structure−function mechanisms subserving other members of this protein superfamily.

A number of experimental approaches have been employed to identify the ligand binding site of the nAChR. The N-terminal extracellular domain (ECD) of the α-subunits contains major determinants for the binding of agonists, such as ACh and carbamylcholine, and competitive antagonists, such as α-bungarotoxin (Bgtx) and *d*-tubocurarine (*1*, *3*, *4*). Three distinct regions of primary sequence involving amino acids 93, 149−151, and 190−198 contribute to ACh binding consistent with a multiple-loop structural model for the site (*5*, *6*). Studies using proteolytic (*7*) or synthetic (*8*, *9*) fragments from the α-subunit, or fusion proteins containing α-subunit sequences (*10*), have shown that residues 173−204 are important for Bgtx binding. The overlap in binding sites for ACh and Bgtx implies that elucidation of the molecular architecture of the Bgtx binding site will provide

† This work was supported by Research Grants GM32629 and NS34348 (E.H.) from the National Institutes of Health. NMR instrumentation was provided for by grants 1S10-RR-08240 from the National Institutes of Health and DBI-N923282 from the National Science Foundation. M.A.G. and L.N.G. were supported in part by National Institutes of Health Predoctoral Training Grant GM07601. M.A.G. was a 1997 recipient of a Pre-Doctoral Fellowship from the Pharmaceutical Research and Manufacturers of America Foundation. This work was done in partial fulfillment of the requirements for a Ph.D. degree from Brown University (M.A.G.).

* Address correspondence to this author. Telephone: 401-863-1034. Fax: 401-863-1595. E-mail: Edward_Hawrot@brown.edu.

‡ Current address: Department of Chemistry, University of New England, Biddeford, ME.

[1] Abbreviations: ACh, acetylcholine; Bgtx, α-bungarotoxin; β-Me, 2-mercaptoethanol; BSA, bovine serum albumin; CD, circular dichroism; DEAE, diethylaminoethyl; DPC, dodecylphosphocholine; DTT, dithiothreitol; ECD, extracellular domain; EDTA, ethylenedinitrilotetraacetic acid; HSQC, heteronuclear single quantum coherence; IC$_{50}$, inhibition constant, 50%; nAChR, nicotinic acetylcholine receptor; nAChRs, nicotinic acetylcholine receptors; NMR, nuclear magnetic resonance; PBS, phosphate-buffered saline; PCR, polymerase chain reaction; PVDF, poly(vinylidene difluoride); SDS, sodium dodecyl sulfate; UV, ultraviolet.

10.1021/bi983007q CCC: $18.00
Published on Web 07/27/1999

valuable structural insights into a major portion of the agonist binding site.

In addition to three "loops" from the α-subunit, biochemical studies have implicated additional "loops" being contributed by either the adjacent γ-subunit or the δ-subunit. Residues in the γ- and δ-subunits that appear to be important for ACh binding have been identified (*11, 12*). Additionally, the site-selective binding of antagonists appears to be due to the contribution of heterologous residues from the γ- and δ-subunits. Specific sites differing between the γ- and δ-subunits have been identified to account for the strong site selectivity in *d*-tubocurarine (*13*) and in conotoxin M1 (*14*) binding.

High resolution structural information of the ligand-gated ion channel superfamily remains elusive as efforts to obtain crystals suitable for X-ray crystallographic studies are problematic and the intact receptors are too large for standard analysis by nuclear magnetic resonance (NMR) spectroscopy. Electron diffraction studies of two-dimensional, tubular arrays of nAChRs from *Torpedo marmorata* have yielded a 9 Å resolution three-dimensional receptor structure (*2, 15*) and a 7.5 Å resolution projection structure (*16*) which reveal the general shape of the oligomeric receptor complex and identify extracellular α-helical elements of structure. An NMR-derived structure of a complex formed between Bgtx and a dodecapeptide corresponding to residues 185−196 from the nAChR α-subunit has provided important details of the molecular conformation of a major segment of the toxin-bound receptor peptide (*17*). Nonetheless, without reasonable quantities of homogeneous preparations of either high-quality crystalline or soluble, isotopically labeled nAChR-derived protein, high-resolution structural details of the nAChR will remain unknown.

One approach to preparing samples from integral-membrane proteins for multidimensional NMR analysis is to recombinantly express isotope-labeled fragments corresponding to extracellular or cytoplasmic domains of functional relevance. Using this reductionist strategy, structures of the N-terminal domains of the interferon γ receptor α-chain (*18*) and epithelial E-cadherin (*19*), and the C-terminal pleckstrin homology domain of β-adrenergic receptor kinase 1 (*20*) have been determined. An extension of this approach is to include a native transmembrane-spanning segment in the expressed fragment for insertion into small membrane-mimicking lipid or detergent micelles. Direct correlation of the structures obtained by NMR for hydrophobic membrane-spanning domains in lipid micelles and lipid bilayers has been shown (*21*). High-quality NMR spectra have been obtained for bacteriophage major coat proteins (*22*−*24*), bacterioopsin (*25*), and glycophorin A (*26*) in monodispersed micelle solutions. Previous attempts to recombinantly express truncated fragments of the α-subunit ECD in bacteria as either fusion proteins (*27, 28*) or directly (*9*) have resulted in either low levels of purified, expressed protein or expressed protein that required detergent solubilization from inclusion bodies. Expression of the entire N-terminal ECD of the mouse muscle-type α-subunit tethered to a cleavable membrane anchorage sequence in stably transfected mammalian cells was recently reported (*29*). The amounts of protein produced by this procedure (10−100 μg) are not sufficient for detailed structural analysis. Bacterial expression and renaturation of the N-terminal ECD of the *Torpedo marmorata* α-subunit from inclusion bodies have been reported (*30*). While the refolded protein binds Bgtx with a K_D of 4 nM, the aggregation state of the protein at millimolar concentrations was not reported. More recently, the bacterial expression and renaturation of the N-terminal ECD of the *Torpedo californica* α-subunit from inclusion bodies have been reported (*31*). However, the renatured protein binds Bgtx with an affinity of ∼130 nM and forms aggregates at micromolar concentrations.

We report here the high-level, soluble expression of two large fragments (αT68His_6 and αT68M1) from the N-terminal extracellular domain of the *Torpedo* α-subunit in *E. coli* at quantities sufficient for structural studies (>12 mg of purified fragment/L of culture). Binding studies provide strong evidence for considerable nativelike structure as all of the structural elements required for high-affinity Bgtx binding are present. The K_D that we obtained for Bgtx binding to the fragments is comparable to that obtained with preparations of the entire N-terminal ECD (*30*), suggesting that the binding of Bgtx to the ECD is entirely due to interaction with residues within the 143−210 region. Circular dichroism (CD) measurements reveal secondary structure components that undergo a cooperative, two-state folding transition upon denaturation by urea. Although the αT68His_6 protein forms soluble aggregates at the concentrations required for detailed NMR studies, a monodispersed preparation of the αT68M1 protein containing the M1 transmembrane domain could be prepared in dodecylphosphocholine (DPC) micelles. The monodispersed αT68M1 preparation demonstrates high-affinity ligand binding in solution binding studies and considerable secondary structure as determined by CD analysis. A similar monodispersed preparation of the αT68M1 fragment could be prepared in sodium dodecyl sulfate (SDS) micelles. The preliminary one-dimensional ^1H and two-dimensional heteronuclear NMR spectra of ^{15}N-labeled αT68M1 in SDS micelles suggest significant structural stability of the micelle-incorporated protein. The results of these initial studies underscore the great potential of this preparation for facilitating additional detailed structural studies of this important receptor region by heteronuclear NMR methods.

EXPERIMENTAL PROCEDURES

Design of TrxFusSSαT68His_6 and TrxFusαT68M1 Plasmids. A synthetic gene encoding *Torpedo* α-subunit residues 159−204 was assembled from six overlapping oligonucleotides in order to incorporate codons preferentially utilized by *E. coli*. All oligonucleotides were synthesized (Applied Biosystems 394 DNA synthesizer), purified by polyacrylamide/urea gel electrophoresis, eluted in 0.5 M ammonium acetate, and desalted over C_{18} SepPak (Millipore) columns. Molecular cloning experiments were performed by standard methods (*32*). In two separate sequential rounds of polymerase chain reaction (PCR) addition, the αT159−204 synthetic gene was extended to encode *Torpedo* α-subunit residues 143−204 and to add an N-terminal thrombin recognition sequence (LVPR/GS). Engineered *Bam*HI and *Sal*I restriction sites flanking the synthetic gene facilitated subcloning into the pTrxFus (Invitrogen) expression plasmid, yielding TrxFusαT62. For the TrxFusSSαT68His_6 construct, the synthetic gene was extended by PCR addition to encode residues 143−210 and a C-terminal six-histidine residue

affinity tag (NGHHHHHH). Engineered *Bam*HI and *Xho*I flanking restriction sites facilitated subcloning into a modified pTrxFus expression vector, pTrxFusSS, that was digested at the complementary *Bam*HI and *Sal*I restriction sites. In the modified pTrxFusSS expression vector, the two cysteine residues present in the thioredoxin fusion protein (C33, C36) were mutated to serine residues through site-directed PCR mutagenesis.

For the TrxFusαT68M1 construct, two additional overlapping oligonucleotides were used to construct a double-stranded cassette encoding *Torpedo* α-subunit residues 195−238, including transmembrane domain M1. This coding sequence was digested with *Eco*VI and *Sal*I and ligated into similarly digested TrxFusαT62 plasmid. Oligonucleotides designed for the addition of the M1 encoding synthetic gene sequence were synthesized (Gibco BRL) and purified as described above. All constructs were transformed into electrocompetent *E. coli* GI724 cells. Positive transformants were screened for the synthetic gene by PCR of tooth-picked colonies using primers complementary to adjacent plasmid sequences or by restriction digestion analysis of isolated transformant plasmid DNA to confirm mutagenesis and gene additions. Sequences were verified using either the Sequenase Version 2.0 Dideoxy Termination (USB) or the DyeDeoxy Terminator (Perkin-Elmer) method.

Expression and Purification of the TrxFusSSαT68His$_6$ and TrxFusαT68M1 Fusion Proteins. The TrxFusSSαT68His$_6$ (23.4 kDa) and TrxFusαT68M1 (25.6 kDa) fusion proteins were overexpressed in *E. coli* cells grown in M9 minimal media. Starter cultures were grown overnight in 50 mL of M9 minimal media supplemented with 100 μg/mL ampicillin at 30 °C and then diluted 1:40 into M9 media in a 2 L benchtop fermentor (Virtis). The culture growth was maintained at 30 °C until an optical density ($A_{500\ nm}$) of 0.5−0.6 was reached. L-tryptophan was added to 100 μg/mL to induce expression from the λ P_L promoter, and the culture was grown at 37 °C for 4 h. For ^{15}N-labeling of the TrxFusSSαT68His$_6$ and TrxFusαT68M1 fusion proteins, ammonium chloride in the starter and expression culture media at 1 g/L was replaced with [^{15}N]ammonium chloride (Cambridge Isotopes).

Soluble expressed TrxFusSSαT68His$_6$ fusion protein was isolated as follows. Cells were harvested by centrifugation, resuspended in 80 mL of 20 mM Tris (pH 8.0)/2.5 mM EDTA/1 mM DTT, and lysed by two passages through a French pressure cell at 20 000 psi. The French pressure cell lysate was ultracentrifuged (100000*g*; 60 min; 4 °C), the supernatant containing soluble TrxFusSSαT68His$_6$ fusion protein was batch-treated with DEAE in 50 mM Tris (pH 8.0)/500 mM NaCl to remove nucleic acids, and the soluble fusion protein was isolated by precipitation with ammonium sulfate at 35% saturation. The precipitated protein was recovered by centrifugation (12000*g*; 10 min; 4 °C), resuspended in 50 mM Tris (pH 8.0)/50 mM NaCl, dialyzed against 50 mM Tris (pH 8.0)/50 mM NaCl/5 mM β-Me buffer, and slowly air-oxidized by dialysis against 50 mM Tris (pH 8.0)/50 mM NaCl.

Soluble expressed TrxFusαT68M1 fusion protein was isolated from the supernatant fraction of the French pressure cell lysate after ultracentrifugation (100000*g*; 60 min; 4 °C) using ion-exchange chromatography on Fast Flow Q Sepharose media (Pharmacia). The bound TrxFusαT68M1 fusion protein was eluted from the column at a NaCl concentration of ∼315 mM in 50 mM Tris (pH 8.0) with a 26−40% linear gradient of 1 M NaCl. Fractions containing the TrxFusαT68M1 fusion protein were dialyzed against 50 mM Tris (pH 8.0)/50 mM NaCl.

Thrombin Cleavage and Purification of the αT68His$_6$ and αT68M1 Receptor Fragments. TrxFusSSαT68His$_6$ and TrxFusαT68M1 fusion proteins were diluted to 1 mg/mL in 50 mM Tris (pH 8.0)/50 mM NaCl and aliquoted into 10 mL fractions. One unit of thrombin protease (Boehringer Mannheim) was added per milligram of protein, and the reaction was allowed to proceed for 18 h at room temperature with gentle rotation. Complete thrombin cleavage of the TrxFusαT68M1 fusion protein was achieved by adding SDS to 0.025% and an additional 0.5 unit of thrombin per milligram of protein and allowing the reaction to continue for another 8 h. For purification of the αT68His$_6$mer receptor fragment, the thrombin reaction products were diluted to 0.25 mg/mL, treated for 2 h with 4 M urea/100 mM DTT/2.5 mM EDTA/10% EtOH, and then applied to a 2 L size-exclusion column of Sephacryl S200 HR media (Pharmacia) equilibrated to 3 M urea/10 mM DTT/2.5 mM EDTA/10% EtOH in 63 mM NH_4HCO_3 (pH 7.0) buffer. Fractions containing pure αT68His$_6$mer protein (9.3 kDa) were collected and dialyzed against either 20 mM Tris (pH 7.0)/5 mM β-Me buffer or 63 mM NH_4HCO_3 (pH 7.0)/5 mM β-Me buffer and then slowly air-oxidized by continued dialysis in the absence of reducing agent. Concentrated samples (micromolar range) of the αT68His$_6$mer fragment were prepared by stirred-cell ultrafiltration (Amicon). For purification of the αT68M1mer receptor fragment, the thrombin reaction products were directly applied to a Sephacryl S300 HR size-exclusion column equilibrated with 50 mM Tris (pH 8.0)/50 mM NaCl. Fractions containing purified αT68M1mer protein (11.5 kDa) were collected and concentrated to micromolar levels by stirred-cell ultrafiltration.

Protein Determination and Electrophoresis. The DC Protein Assay (BioRad), a modified Lowry assay (*33*), was used for all protein concentration determinations. SDS−polyacrylamide gel electrophoresis was performed using 15% (w/v) Tris−polyacrylamide gels in the system of Laemmli (*34*). For improved resolution of proteins under ∼10 kDa in molecular mass, samples for electrophoresis were applied to 16.5% Tricine−polyacrylamide gels as described (*35*).

N-Terminal Amino Acid Sequencing. Purified αT68His$_6$ and αT68M1 proteins were resolved on 15% SDS−polyacrylamide gels and electroblotted onto PVDF membranes. The protein band visible by Coomassie staining was excised and analyzed by an Applied Biosystems 494 cLC sequencer (Yale University).

Equilibrium ^{125}I-Bgtx Binding Determinations. Approximately 250 fmol of the purified αT68His$_6$ and αT68M1 proteins diluted in 100 μL of 15 mM Na_2CO_3/35 mM $NaHCO_3$ buffer (*36*) was coated onto microtiter plate wells overnight (Nunc, Maxisorb); or ∼65 fmol of AChR-enriched *Torpedo* membranes, prepared as described (*37*), was plated onto the wells of a microtiter plate in 100 μL of 10 mM NaH_2PO_4 (pH 7.4)/150 mM NaCl (PBS) by centrifugation at 1000*g*. The wells were aspirated and incubated for 1 h in 200 μL of 2% BSA in 5 mM glycine (pH 7.5). The wells were aspirated and incubated for 20 h at 25 °C in increasing concentrations of ^{125}I-Bgtx (Dupont NEN) diluted with

unlabeled Bgtx (RBI) to a known specific activity in 100 μL of 5 mM glycine (pH 7.5)/0.2% BSA. Glycine buffer was used in all Bgtx binding studies, unless otherwise specified, to avoid the competitive action of inorganic cations (e.g., Na^+, K^+, and Ca^{2+}). The cation sensitivity of Bgtx binding to the native nAChR has been described previously (*38*). A 75 μL aliquot was taken from each well to determine the unbound (free) radioactivity. Wells were aspirated and washed 4 times with 200 μL of 5 mM glycine (pH 7.5)/0.2% BSA, and the bound radioactivity was determined. Nonspecific binding, determined in the presence of 20 μM unlabeled Bgtx, was subtracted from the total binding. Each data point is the mean of triplicate determinations.

^{125}I-Bgtx Binding Dissociation Rate Determinations. Approximately 2.5 pmol of the purified αT68His_6 and αT68M1 proteins diluted in 100 μL of 15 mM Na_2CO_3/35 mM $NaHCO_3$ buffer (*36*) was coated onto microtiter plate wells overnight (Nunc, Maxisorb); or ~0.2 pmol of AChR-enriched *Torpedo* membranes, prepared as described (*37*), was plated onto the wells of a microtiter plate in 100 μL of 10 mM NaH_2PO_4 (pH 7.4)/150 mM NaCl (PBS) by centrifugation at 1000*g*. Wells were aspirated, and 200 μL of 2% BSA quench solution was added. Following incubation for 1 h at room temperature, wells were aspirated, washed twice with 5 mM glycine (pH 7.5)/0.2% BSA, and incubated for 20 h at room temperature in 100 μL of 8 nM ^{125}I-Bgtx. Dissociation was initiated by the addition of 10 μM unlabeled Bgtx, and at specific time intervals thereafter, wells were aspirated and washed 4 times with 200 μL of 0.2% BSA in 5 mM glycine (pH 7.5), and the bound radioactivity was determined. Nonspecific ^{125}I-Bgtx binding was measured in the presence of 10 μM unlabeled Bgtx during equilibrium binding. All data points represent triplicate determinations.

Solid-Phase Competition Binding Determinations. Competition binding assays were essentially carried out as described previously (*39*). Briefly, 1.0 μg of AChR-enriched *Torpedo* membranes, prepared as described (*37*), was plated onto the wells of a microtiter plate in 100 μL of 10 mM NaH_2PO_4 (pH 7.4)/150 mM NaCl (PBS) by centrifugation at 1000*g*; or 0.25 μg of purified receptor fragment protein diluted in 100 μL of 15 mM Na_2CO_3/35 mM $NaHCO_3$ buffer (*36*) was plated overnight. Wells were aspirated, and 200 μL of 2% BSA quench solution was added. Following incubation for 1 h at room temperature, wells were aspirated, washed twice with 5 mM glycine (pH 7.5)/0.2% BSA, and incubated for 2 h at room temperature in 100 μL of 3 nM ^{125}I-Bgtx plus varying concentrations of unlabeled competitor ligand: Bgtx, curare, carbachol, or nicotine in 5 mM glycine (pH 7.5)/0.2% BSA. Wells were aspirated and washed 4 times with 200 μL of 0.2% BSA in 5 mM glycine (pH 7.5), and the radioactivity was determined. The competition curves and resulting IC_{50} values were derived by logistic equation curve-fitting using Origin 4.1 software (Microcal).

Competition between Solubilized αT68M1 Peptide and Native AChR for ^{125}I-Bgtx Binding. Competition binding between the αT68M1mer and native AChR from *Torpedo* membranes was carried out as previously described (*40*). Briefly, 1.25 nM ^{125}I-Bgtx was incubated with 5 nM−5 μM concentrations of αT68M1 peptide/DPC (1:500 molar ratio of peptide to DPC) in 0.2% BSA overnight at 25 °C. Wells of a microtiter plate were coated with 375 ng of AChR-enriched *Torpedo* membranes, prepared as described (*37*), in 100 μL of PBS by centrifugation at 1000*g*. Following aspiration, the peptide−Bgtx mixture was added to the wells for a 6 min incubation at 25 °C. The wells were aspirated and washed 4 times with 0.2% BSA/PBS, and the radioactivity bound to the wells was determined. Nonspecific ^{125}I-Bgtx binding was measured in the presence of 10 μM unlabeled Bgtx, and found to be <3% of the total binding. All data points represent triplicate determinations.

Molecular Size Analysis of Oligomeric States. Assessment of the aggregation state of the fusion proteins and purified receptor fragments was made using size-exclusion chromatography on Sephacryl S200 HR media developed under nondenaturing conditions. For molecular weight estimations, the elution volume of the protein of interest was compared to the elution volumes of a set of gel-filtration molecular weight determination marker proteins. Further size determinations of the SDS and DPC micelle solubilized αT68M1 purified fragment were made using a Protein Solutions laser light scattering instrument at the University of Edinburgh.

Circular Dichroism Analysis. Spectra were collected using a double-beam OLIS XL450 spectrometer. The spectrometer was calibrated using a standard of D-(+)-10-camphorsulfonic acid. Cuvettes with path lengths of 0.01−0.1 cm were used, and data points were collected at 1 nm intervals with a 3 s delay time. Spectra were recorded at 25 °C unless otherwise noted from 250 to 190 nm, and the mean residue ellipticity (degrees centimeter squared per decimole) was determined. Each spectrum represents the average of three scans and was corrected for light scattering by buffer subtraction. Secondary structure content was estimated using the Convex Constraint Algorithm (*41*).

Preparation of αT68His_6mer and αT68M1mer Samples for NMR Spectroscopy. Samples of the αT68His_6mer receptor fragment at 0.4 mM concentrations in 63 mM ammonium bicarbonate (pH 7.0) were prepared using BioMax-5 concentrator devices (Millipore) at 3000*g*. Samples of the αT68M1mer receptor fragment for NMR were prepared either by adding a molar excess of SDS-d_{25} (Cambridge Isotopes) to purified αT68M1 protein in 50 mM Tris (pH 8.0)/50 mM NaCl prior to a buffer exchange into 50 mM NaH_2PO_4 (pH 4.5) on size-exclusion PD-10 media (Pharmacia) or as described previously (*42*). Protein solutions were concentrated using Centriplus-3 devices (Amicon), and final NMR samples were filtered through a cellulose acetate (0.45 μm) syringe filter (Millipore). D_2O (Cambridge Isotopes) was added to 10%.

NMR Data Acquisition. NMR spectra were acquired on Bruker DRX400 and DRX600 spectrometers equipped with AVANCE consoles and pulse-field gradients. For two-dimensional experiments, quadrature detection in t_1 employed the phase-sensitive method of States-TPPI (*43*). ^{1}H−^{15}N heteronuclear single quantum coherence (HSQC) spectra of the αT68M1 protein were acquired at 45 °C for DPC samples and at 50 °C for SDS samples using a gradient-enhanced HSQC pulse sequence (*44*) with ^{15}N decoupling during the acquisition period using GARP (*45*) and a WATERGATE sequence (*46*) for water suppression. The ^{1}H observe and ^{15}N sweep widths were 12.5 and 35 ppm, respectively. Proton chemical shifts are relative to the water signal (4.7 ppm), and ^{15}N chemical shifts are relative to external ammonia. Spectra were collected with 2048 real data points in the t_1

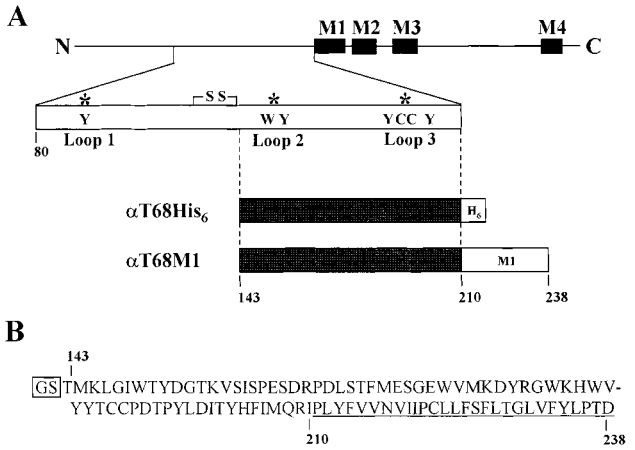

FIGURE 1: Schematic representation and amino acid sequence of the α-subunit fragments αT68His$_6$ and αT68M1 based on the sequence from *Torpedo californica*. (A) One-third of the extracellular domain, residues 143−210, including the agonist binding site containing subdomains, loop 2 and loop 3 (*3*), and the major determinant for Bgtx binding, residues 173−204, are included in each receptor fragment. (B) The amino acid sequence of the αT68M1 fragment. The underlined sequence corresponds to the first transmembrane domain M1, which extends from residues 211−237, and includes a terminal aspartate residue (Asp^{238}). The sequence of the αT68His$_6$ fragment is identical except that the underlined M1 sequence is replaced by NGHHHHHH, a six histidine residue affinity tag. Liberation of the receptor fragments from the thioredoxin fusions by thrombin protease leaves two unauthentic residues, GS, at the N-termini.

dimension and 256 increments in t_2. Using Bruker XWIN-NMR software (Version 1.2) for data processing, the data were expanded to 1024 (^{15}N) using linear prediction and processed with Gaussian apodization functions for resolution enhancement.

RESULTS

Expression and Purification of αT68His$_6$ and αT68M1 Proteins in E. coli. We prepared two synthetic gene constructs encoding residues α143−210 from the N-terminal extracellular domain of the α-subunit from *Torpedo californica* (Figure 1). To enhance the soluble expression of the receptor fragments, a synthetic gene was designed from amino acid sequence back-translation and incorporation of codons preferentially utilized in *E. coli* (*47*). The receptor fragments contain 30% of the N-terminal domain of the α-subunit and include two of the three important "loop" regions that are believed to contribute to the agonist binding site (*6, 48*). αT68His$_6$ contains a C-terminal poly-histidine residue affinity tag (HHHHHH) that is positioned adjacent to a hydroxylamine chemical cleavage site (NG) to allow for removal of the tag, if necessary (Figure 1B). αT68M1 includes the first transmembrane domain M1 from the α-subunit (Figure 1B), residues α211−237, and a terminal aspartate residue, Asp^{238}, and was designed to allow fragment tethering through the M1 domain to lipid or detergent micelles. The receptor fragment genes were appended to the C-terminus of the gene for *E. coli* thioredoxin in the expression vector pTrxFus or a modified version containing serine substitutions of the two cysteines in thioredoxin, pTrxFusSS. To allow for the liberation of the receptor fragments from thioredoxin, we utilized a thrombin protease recognition site (LVPR/GS).

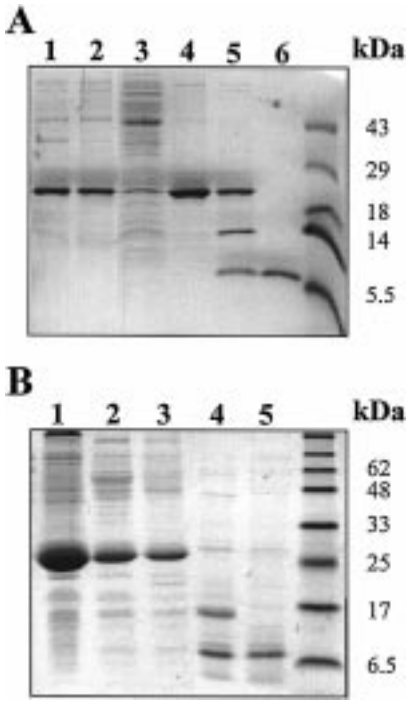

FIGURE 2: Isolation and purification of the αT68His$_6$ (A) and αT68M1 (B) fragments overexpressed in *E. coli*. (A) 15% SDS−PAGE of αT68His$_6$ at various stages of purification. Samples analyzed were *E. coli* crude cell lysate (lane 1), soluble supernatant fraction (lane 2), soluble fraction of ammonium sulfate precipitation (lane 3), ammonium sulfate precipitated fusion protein (lane 4), products of thrombin cleavage (lane 5), and gel-filtration (Sephacryl) purified αT68His$_6$ fragment (lane 6). (B) 15% SDS−PAGE of αT68M1 at various stages of purification. Samples analyzed were *E. coli* crude cell lysate (lane 1), soluble supernatant fraction (lane 2), Fast Flow Q Sepharose isolated fusion protein (lane 3), products of thrombin cleavage (lane 4), and gel-filtration (Sephacryl) purified αT68M1 fragment (lane 5). Proteins were stained with Coomassie Brilliant Blue, and molecular mass markers are indicated at the right in kDa.

The TrxFusSSαT68His$_6$ (23.4 kDa) and TrxFusαT68M1 (25.6 kDa) fusion proteins were overexpressed in *E. coli* GI724 cells grown in M9 minimal media. Both the total crude extracts and the soluble, high-speed centrifugation supernatants from induced cultures show high expression levels of the receptor fragment-containing fusion proteins (Figure 2). As judged by SDS−polyacrylamide gels and protein determinations of the various fractions, greater than 80% of the recombinant TrxFusSSαT68His$_6$ and 60% of the recombinant TrxFusαT68M1 fusion proteins were recovered in the supernatant fraction following centrifugation of French press extracts at 100000*g*.

Although the TrxFusSSαT68His$_6$ fusion protein could be purified using a nickel affinity column, we obtained the highest yields of soluble fusion protein by following an ammonium sulfate precipitation scheme. This procedure typically resulted in ∼250 mg of the TrxFusSSαT68His$_6$ fusion protein from a 2 L benchtop fermentor culture at greater than 95% purity as judged by SDS−polyacrylamide gels (Figure 2A). To isolate soluble TrxFusαT68M1 fusion protein from the high-speed centrifugation supernatant, anion exchange chromatography on Fast Flow Q Sepharose (Pharmacia) was most reliable and effective. We typically obtained ∼190 mg of TrxFusαT68M1 fusion protein from a 2 L

benchtop fermentor culture at 90% purity as judged by SDS−polyacrylamide gels (Figure 2B).

The analysis by standard high-speed centrifugation criteria had demonstrated that both receptor fragment-containing fusion proteins were soluble. Additional studies were pursued and showed that both fusion proteins self-associated as large but soluble aggregates. For example, in sucrose gradient centrifugation studies, the TrxFusSSαT68His$_6$ protein sedimented in the molecular mass range of 440−660 kDa. Nonetheless, the receptor fragments could be released from the recombinant fusion protein preparation following treatment with the purified protease, thrombin. A large fraction (∼50%) of the αT68His$_6$ receptor fragment (9.3 kDa) could be liberated from its fusion partner, but efforts to further enhance the efficiency of thrombin cleavage were unsuccessful. In contrast, liberation of the αT68M1 receptor fragment (11.5 kDa) by thrombin was 95% complete under the same conditions and could be further improved to 100% cleavage with the addition of 0.025% SDS and fresh thrombin.

Monomeric αT68His$_6$ receptor protein was isolated by size-exclusion chromatography on Sephacryl S200 HR media in the presence of urea and DTT. Due to the tendency of the αT68His$_6$mer to associate with the uncleaved fusion protein, efficient separation required partially denaturing and reducing conditions. Approximately 25 mg of purified soluble αT68His$_6$ receptor protein was typically isolated from a 2 L benchtop fermentor culture. Purified αT68M1 receptor protein was also isolated by size-exclusion chromatography, but in contrast to the αT68His$_6$mer, Sephacryl S300 HR gel filtration under nondenaturing conditions and in the absence of detergents easily separated the self-associated but still soluble receptor fragment from thioredoxin. We typically isolated ∼27 mg of purified soluble αT68M1 receptor protein from a 2 L benchtop fermentor culture. Substitution of [^{15}N]-ammonium chloride in the M9 minimal media to incorporate ^{15}N into the receptor fragment-containing fusion proteins did not alter the expression levels, purification protocols, or final yields of the receptor fragment proteins. N-Terminal protein microsequencing confirmed the specificity of thrombin cleavage at the expected N-terminal arginine (LVPR/GS) and the identity of the isolated receptor fragments. Therefore, both preparations have proved to be amenable to the production of milligram quantities of receptor fragments as would be required for detailed structural studies.

High-Affinity Binding of ^{125}I-Bgtx to the Purified αT68His$_6$ and αT68M1 Proteins. To establish the functional integrity of the αT68His$_6$ and αT68M1 receptor proteins, binding affinities for the nAChR antagonist Bgtx were determined in solid-phase equilibrium binding studies (Figure 3). ^{125}I-Bgtx binding to the αT68His$_6$ and αT68M1 receptor proteins was saturable with K_D values of 3.3 and 2.7 nM, respectively. Under identical assay conditions, the native receptor in *Torpedo* membranes demonstrated saturable ^{125}I-Bgtx binding with a K_D value of 1.3 nM. Scatchard analysis of the data indicated that the purified receptor proteins contain a single class of equivalent and independent binding sites (Figure 3, insets). Based on the B_{max} values obtained in these assays, the fraction of applied protein that bound ^{125}I-Bgtx was determined to be 30% for the αT68His$_6$ fragment and 46% for the αT68M1 fragment. In addition, we compared the dissociation kinetics for ^{125}I-Bgtx bound to the receptor proteins to that of the native receptor in *Torpedo* membranes using a solid-phase assay (data not shown). For the native receptor, the initial dissociation phase determined following the addition of unlabeled Bgtx exhibited a half-time of 6.5 h. Under identical conditions, we determined half-times of 3.8 and 3.9 h for the αT68His$_6$ and αT68M1 receptor proteins, respectively.

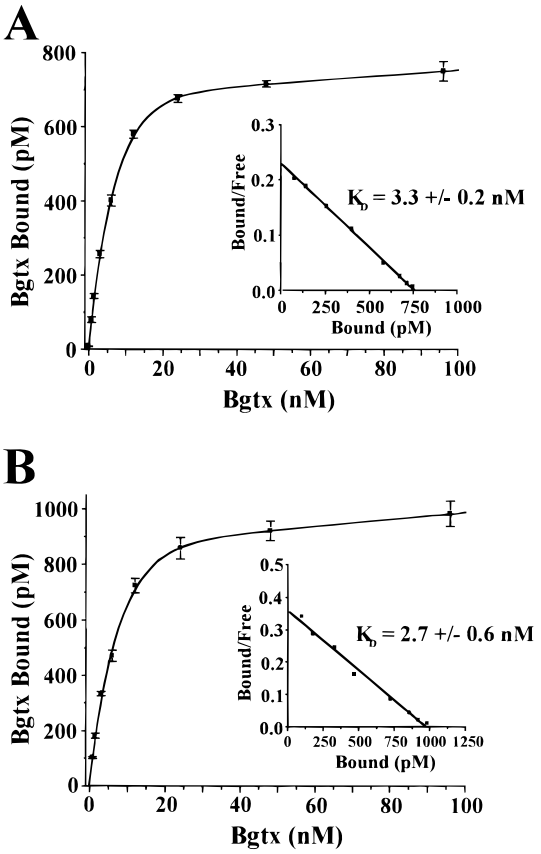

FIGURE 3: Saturation binding of ^{125}I-Bgtx to purified αT68His$_6$ (A) and αT68M1 (B) fragments. Purified recombinant protein (∼0.25 pmol) was plated onto microtiter plates and incubated with various concentrations of ^{125}I-Bgtx for 20 h. The wells were washed, and the bound radioactivity was counted. For specific binding, nonspecific binding in the presence of 20 μM Bgtx was subtracted from the total binding. Each data point is the mean of triplicate determinations. Scatchard transformations of the data are shown in the insets.

Binding Affinities of the Purified αT68His$_6$ Protein for Other Cholinergic Ligands. The αT68His$_6$ protein exhibits strong ligand binding activities in solid-phase competition binding assays with ^{125}I-Bgtx (Figure 4). The binding activities are reported as IC_{50} values, the ligand concentration that competes 50% of the total ^{125}I-Bgtx binding. IC_{50} values obtained for Bgtx competition with the purified receptor fragment were nearly identical to that of native nAChR from *Torpedo* membranes assayed in the same experiment. The expressed fragments, fully functional in terms of Bgtx binding, appear to consist of a structurally homogeneous population of binding sites based on the competition curves. The αT68M1 protein also exhibits IC_{50} values for Bgtx that are similar to that of the native AChR from *Torpedo* membranes in identical solid-phase assays (data not shown). Assays with the αT68His$_6$ peptide using curare and carbamylcholine as competitors yield IC_{50} values of 110 μM and 8.5 mM, respectively (Figure 4). In identical experiments, the measured IC_{50} value for nicotine was 200 μM (data not shown).

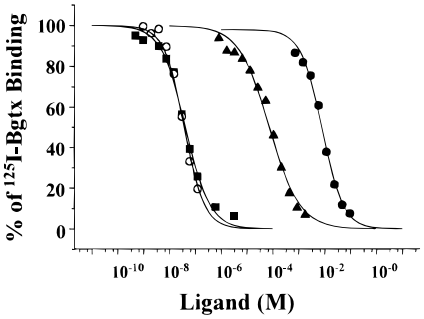

FIGURE 4: Solid-phase competition binding assays with ^{125}I-Bgtx. Competition of ^{125}I-Bgtx binding to native nAChRs from *Torpedo* membranes by unlabeled Bgtx (■), or to purified αT68His$_6$ protein by unlabeled Bgtx (○), curare (▲), and carbachol (●). Wells of microtiter plates were coated with 1 μg of *Torpedo* electric organ membranes or 0.25 μg of αT68His$_6$ protein and incubated with 3 nM ^{125}I-Bgtx plus various concentrations of unlabeled ligand. After a 2 h incubation, wells were washed, and the bound radioactivity was determined. The IC$_{50}$ values, determined by nonlinear curve fitting of the data, are 38.0 nM (■), 43.5 nM (○), 110 μM (▲), and 8.5 mM (●), respectively.

K_I values were calculated from the above IC$_{50}$ concentrations for competing ligands according to Cheng and Prusoff (*49*) and were determined to be 58 μM, 4.5 mM, and 105 μM, respectively, for curare, carbamylcholine, and nicotine.

Characterization and Secondary Structure Analysis of the αT68His$_6$ Protein. The αT68His$_6$ receptor fragment at protein concentrations at or below ~20 μM was monomeric as demonstrated by size-exclusion chromatographic analysis on Sephacryl S200 HR media under nondenaturing conditions (Figure 5A). The solubility of monomeric αT68His$_6$mer was sufficient for ligand binding studies and analysis of secondary structure by CD; however, at the higher concentrations necessary for NMR studies, the protein self-associated to form large although soluble aggregates. In solid-phase competition binding studies with ^{125}I-Bgtx, the isolated monomeric form of the αT68His$_6$mer has the same apparent affinity (IC$_{50}$) for Bgtx as the aggregated form of the protein (data not shown). The CD spectrum of monomeric αT68His$_6$-mer, which provides information on protein secondary structure, indicated that the αT68His$_6$mer contains a small amount of α-helical structure (13%) and significant β-sheet structure (39%) as shown in Figure 5B. The αT68His$_6$mer exhibited a concentration-dependent variation in secondary structure composition indicative of self-association at elevated protein concentrations. For example, at protein concentrations of 200 and 100 μM, the CD spectra of the αT68His$_6$mer were dominated by a significant β-sheet component with a single minimum ellipticity at ~214 nm. When diluted to concentrations of 20 and 4 μM, the CD spectra, in contrast, revealed a greater apparent α-helical content with dual ellipticity minima at 208 and 220 nm. Urea denaturation of the purified αT68His$_6$mer (at 20 μM) as measured by CD analysis at 222 nm was used to probe the structural content of the isolated receptor fragment. The results obtained are consistent with a cooperative, two-state folding transition where 50% of the maximal change in ellipticity at 222 nm was observed at 3.0 M urea (Figure 5B, inset).

Circular Dichroism and Laser Light Scattering Analysis of the αT68M1 Protein. As micelles have been useful in the structural investigation of a variety of membrane proteins

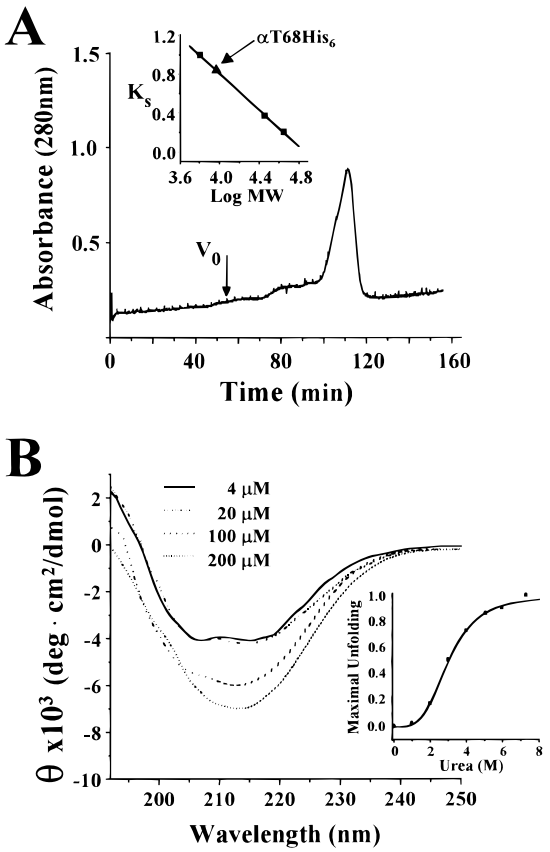

FIGURE 5: Characterization of the purified αT68His$_6$mer protein. (A) Gel-filtration chromatography profile of purified and renatured αT68His$_6$ fragment at 0.15 mg/mL on Sephacryl S200 HR media in 20 mM Tris (pH 7.0), 50 mM NaCl buffer at a 2 mL/min flow rate. Absorbance of the eluted protein was monitored at 280 nm. The calculated size of αT68His$_6$mer, determined by comparison of the elution volume to that of molecular weight standards (shown in the inset), is ~9 kDa as expected for the monomeric form of the protein. (B) CD study of the purified αT68His$_6$mer at varying protein concentrations: 200, 100, 20, and 4 μM as indicated in the figure. Inset: Denaturation of the monomeric αT68His$_6$ fragment by urea. The mean residue ellipticity (θ) of the αT68His$_6$ monomer was measured by CD at 222 nm upon additions of urea. Each spectrum, the average of three scans, was recorded at 25 °C.

(*50*) that otherwise form aggregates in solution, we investigated whether the 68mer could be anchored onto DPC or SDS micelles via insertion of the M1 transmembrane domain. SDS and DPC have both been shown to be excellent membrane mimetics and provide an environment for the insertion of hydrophobic membrane spanning domains (*21, 22, 51*). Gel filtration analysis and laser light scattering measurements revealed that the purified αT68M1 fragment self-associates into an aggregate (molecular mass > 1500 kDa) even at micromolar concentrations. The self-associated form of the αT68M1 fragment is characterized by significant β-sheet secondary structure as determined by CD analysis (Figure 6A). As increasing amounts of DPC are added, the resulting CD spectra show saturable increases in ellipticity at 209 and 222 nm wavelengths. CD minima at these two wavelengths are usually indicative of α-helical secondary structure (*52*). These observations are consistent with the M1 domain inserting into the hydrophobic lipid environment and assuming an α-helical conformation. Qualitatively similar results were observed in the CD spectra of αT68M1 upon the addition of increasing amounts of SDS.

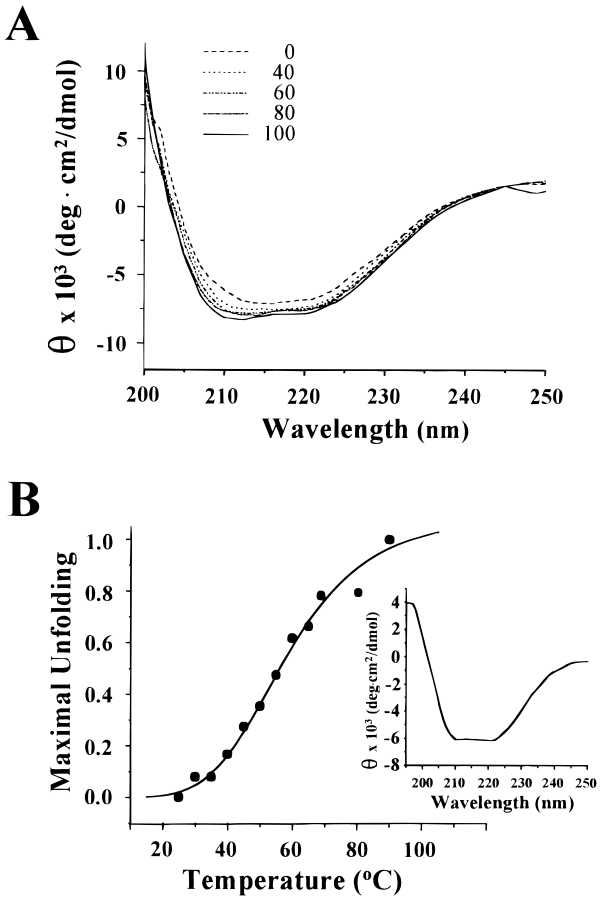

FIGURE 6: Structural analysis of the purified αT68M1 fragment in DPC micelles. (A) CD spectra obtained with the αT68M1 fragment at 80 μM and titrated with an increasing molar excess of DPC. The mean residue ellipticity (θ) of the αT68M1 protein was observed from 190 to 250 nm. Each curve is the average of three separate scans. The molar fold excess of DPC that was added is indicated in the figure. (B) Thermal denaturation of the αT68M1 fragment (0.25 mM protein concentration in a 500-fold molar excess of DPC) followed by measuring the CD signal at 222 nm and at temperatures ranging from 25 to 90 °C. Maximal unfolding was determined by the change in CD signal at 222 nm observed after increasing the temperature from 25 to 90 °C. Inset: CD spectrum of the αT68M1mer at 0.25 mM in DPC micelles (500-fold molar excess of DPC) in 50 mM sodium phosphate (pH 4.7) buffer.

In concordance with these CD studies, we performed dynamic laser light scattering measurements on a αT68M1/DPC micelle mixture which indicated that 96% of the particles have an apparent molecular mass of ~28 kDa. The concentration of DPC in this sample was 49 mM, approximately 25 times the critical micelle concentration (*53*). As this finding indicates that 1 molecule of receptor fragment (11.5 kDa) is most likely associated with ~42 molecules of DPC, we have obtained an essentially monodisperse preparation of αT68M1 fragment incorporated into DPC micelles. Previous biophysical studies have determined that DPC forms small micelles of ~56 monomers in the absence of protein (*54*). Our data are consistent with these studies as we anticipate that the M1 domain displaces a number of lipid molecules. Qualitatively similar results were observed for a sample of the αT68M1 fragment in SDS micelles. Approximately 97% of the particles have an apparent molecular mass of ~26 kDa at SDS concentrations of 82 mM, approximately 10 times the critical micelle concentration

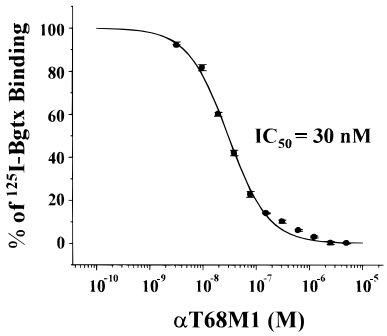

FIGURE 7: Determination of ^{125}I-Bgtx binding by the αT68M1 fragment in DPC micelles (500-fold molar excess of DPC). Various concentrations of the αT68M1/DPC mixture were preincubated with 1.25 nM ^{125}I-Bgtx overnight. Aliquots taken from these incubations were added to microtiter wells containing 375 ng of nAChR *Torpedo* membranes to determine the amount of ^{125}I-Bgtx depletion by micelle-incorporated αT68M1. The concentration of αT68M1 that results in a 50% decrease in ^{125}I-Bgtx binding to the receptor was measured under initial rate conditions where binding to the native receptor is linearly dependent on Bgtx concentration.

(*53*). There was no evidence of denaturation of the αT68M1mer in DPC as CD studies failed to indicate any random coil formation in the presence of a 500-fold molar excess of DPC (Figure 6B, see inset). Likewise, in the presence of up to a 1000-fold molar excess of SDS, there was no evidence of denaturation of the αT68M1mer by CD studies (data not shown). Unfolding of the micelle-associated αT68M1 fragment in DPC micelles could, however, be demonstrated following heating as we observed incremental positive changes in ellipticity during heating, most notably at the canonical α-helical wavelength of 222 nm, as shown in Figure 6B.

Solution Binding Characteristics of the Micelle-Dispersed αT68M1 Protein. To further establish the nativelike structure of the monodispersed αT68M1 protein in DPC micelles, we measured the ability of αT68M1/DPC preparations to bind Bgtx in solution binding experiments. αT68M1/DPC preparations were preincubated with ^{125}I-Bgtx and then assayed for depletion of free ^{125}I-Bgtx by adding the mixture to AChR-enriched *Torpedo* membranes in a solid-phase assay. We determined the amount of ^{125}I-Bgtx binding to native receptors under initial rate conditions where binding is linearly dependent on the concentration of free ^{125}I-Bgtx. The IC_{50} value obtained is the concentration of micelle-incorporated αT68M1 protein that effectively depletes 50% of the total ^{125}I-Bgtx available to bind to the native AChR. We obtained an apparent IC_{50} of 30 nM for the αT68M1 fragment in DPC micelles (Figure 7).

Heteronuclear NMR Analysis of the Micelle-Dispersed αT68M1 Protein. Several milligrams of ^{15}N-enriched αT68M1 protein dispersed in SDS or DPC micelles were prepared for one- and two-dimensional NMR studies. By examining the ^{1}H spectra (data not shown) and ^{1}H−^{15}N heteronuclear single quantum coherence (HSQC) spectra, we were able to adjust the sample conditions (micelle ratio, salt content, pH, and temperature) to narrow the resonance line widths. NMR spectra were recorded at an elevated temperature to increase the overall rotational correlation time and yield narrower resonance line widths. To minimize amide proton exchange with the solvent, samples were prepared at pH 4.7. The HSQC spectra obtained with either DPC- or SDS-incorpo-

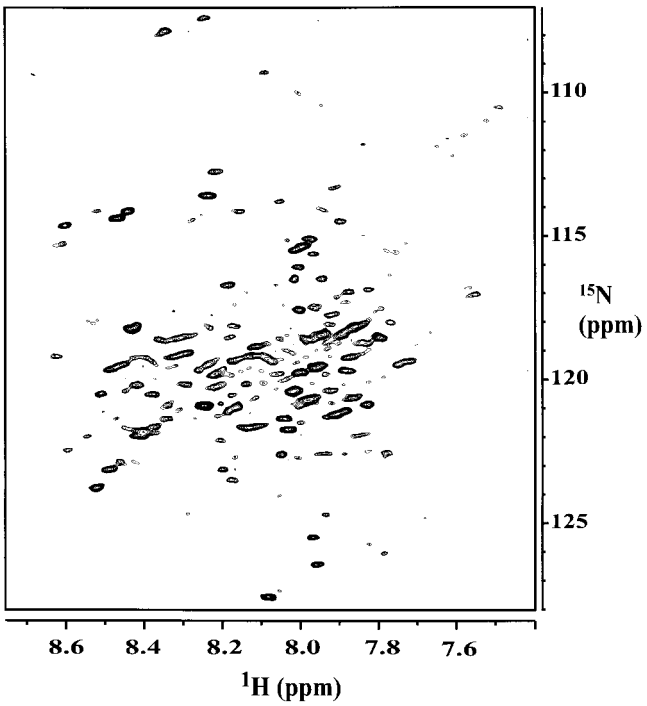

FIGURE 8: Two-dimensional heteronuclear NMR study of the αT68M1 protein in SDS micelles. The ^{1}H−^{15}N HSQC spectrum of the ^{15}N-αT68M1 fragment at 0.5 mM with 250 mM SDS-d_{25} in 50 mM sodium phosphate (pH 4.7), 10% D_2O at 50 °C was recorded on a Bruker AVANCE600 spectrometer. Due to the method of recombinant expression in *E. coli*, the αT68M1 fragment lacks ^{15}N-enriched tryptophan residues.

rated samples were comparable. Figure 8 shows the ^{1}H−^{15}N HSQC spectrum of αT68M1mer prepared in SDS micelles (1000-fold molar excess of SDS) at a protein concentration of 0.5 mM. In this spectrum, the dispersion of cross-peaks is clearly sufficient for us to resolve 70 cross-peaks of the 93 expected cross-peaks from ^{15}N-attached protons. These results provide support that the preparation is indeed monodisperse and are highly indicative of stable structural elements. Indole cross-peaks from tryptophan are not observed in the HSQC spectrum because the expression of TrxFusαT68M1 in *E. coli* was induced by the exogenous addition of L-tryptophan. Tryptophan is not a substrate for *E. coli* transaminase activity (*55*); therefore, only the four tryptophan residues in the recombinant αT68M1 protein should lack isotopic ^{15}N-enrichment. Based on an assessment of the HSQC spectrum, samples of the αT68M1 receptor fragment incorporated into SDS micelles were stable for >1 month. The chemical shifts of the resonances observed in the HSQC spectrum did not change over a temperature range of 25−65 °C (data not shown), further indicating a stable complex.

DISCUSSION

Preparation of Soluble nAChR Fragments Derived from the ECD. We have demonstrated that a fragment corresponding to ∼30% of the ECD from the nAChR α-subunit can be expressed in *E. coli* as a soluble fusion protein at high levels and that it can be proteolytically released from its fusion partner and purified in quantities necessary for high-resolution NMR structure studies. The large-scale purification (>12 mg of purified fragment/L of culture) of nAChR-derived recombinant protein for NMR structural studies was made possible by utilizing a synthetic gene construct for the *Torpedo* α-subunit extracellular region 143−210 appended to the C-terminus of the intracellular oxidoreductase thioredoxin. Several efforts to produce nAChR-derived proteins in *E. coli* for use in structural studies have been previously reported. An α-subunit fragment consisting of residues 122−205 from the mouse nAChR was directly expressed in *E. coli* (*9*, *56*). Smaller α-subunit fragments comprising residues 184−200 and 186−198 (*57*) and 166−211 (*10*) from *Torpedo* were expressed in *E. coli* as C-terminal fusions to the TrpE protein. More recently, the entire ECD of the α-subunit from *Torpedo marmorata* (*30*) and from *Torpedo californica* (*31*) have been expressed in bacteria and renatured from inclusion body preparations. In contrast to those reports, where the expressed protein was found largely in inclusion bodies, the expression strategy described here produces a soluble fusion protein containing nAChR α-subunit sequence. Furthermore, upon proteolytic release from the fusion protein partner, the α-subunit fragment, bearing either a six-residue histidine tag (αT68His$_6$) or the M1 transmembrane domain (αT68M1) on the C-terminus, appears to form a soluble protein that demonstrates nativelike ligand binding properties. Our structural studies of the α-subunit fragments containing residues 143−210 provide the first insights into the biophysical properties of a functionally important domain from the ECD of the nAChR in solution at millimolar concentrations.

The Nativelike, High-Affinity Ligand Binding of the nAChR Fragments. The ligand binding properties exhibited by the purified recombinant receptor fragments provide compelling evidence for nativelike folding and demonstrate that the isolated receptor fragments contain the major structural elements required for Bgtx binding to the native receptor. The purified recombinant receptor fragments αT68His$_6$ and αT68M1 form soluble proteins that exhibit saturable, high-affinity ^{125}I-Bgtx binding with K_D values of 3.3 and 2.7 nM, respectively. Under identical assay conditions, the native receptor in *Torpedo* membranes demonstrates saturable ^{125}I-Bgtx binding with a K_D value of 1.3 nM. The Bgtx affinities exhibited by the receptor fragments are comparable to the range of affinities (0.4−3 nM) reported by others for the intact nAChR from *Torpedo* in solid-phase assays (*58*). The observation that the αT68His$_6$ and αT68M1 fragments bind Bgtx with an affinity identical to that reported for a renatured preparation of the N-terminal ECD of the nAChR α-subunit (4 nM) (*30*) indicates that the region comprising residues 143−210 is responsible for the interaction of Bgtx with the ECD of the α-subunit. No additional interactions with sites N-terminal to residue 143 are required to account for the high-affinity interaction between Bgtx and the ECD of the α-subunit. It is possible that interactions with subunits adjacent to the α-subunit may provide contributions to Bgtx binding to the native receptor (*59*). The Bgtx affinities exhibited by the receptor fragments are 2 orders of magnitude higher than the Bgtx affinity more recently reported for a renatured preparation of the entire ECD of the nAChR α-subunit (∼134 nM) (*31*). The fraction of receptor fragment protein which bound ^{125}I-Bgtx, as derived from the observed B_{max} values, was 30% for αT68His$_6$ and 46% for αT68M1. This is likely to be an underestimate of the fraction of folded protein as it is unknown what percentage of the applied

protein fails to bind to the microtiter wells used in these assays.

Additional evidence indicating that the receptor fragments adopt a nativelike fold was obtained from competition assays where the receptor fragments were characterized by IC_{50} values for Bgtx that were nearly identical to that of the native receptor assayed under identical conditions. Furthermore, we found that the kinetics of dissociation of the ^{125}I-Bgtx/receptor protein complexes were comparable to those of the native receptor in *Torpedo* membranes. For the native receptor, the initial dissociation phase was characterized by a half-time of 6.5 h. We determined half-times of 3.8 and 3.9 h for the αT68His$_6$ and αT68M1 receptor proteins, respectively. In comparison, the half-time of dissociation for a renatured preparation of the entire α-subunit ECD was found to be an order of magnitude lower (∼0.5 h) (*30*). Our finding that the half-times of dissociation are within the same order of magnitude as the intact receptor further argues that the αT68His$_6$ and αT68M1 receptor proteins possess nativelike receptor ligand binding properties. As previously determined half-times for α-neurotoxin dissociation (*60, 61*) obtained with other methods are approximately 1 order of magnitude larger than the values we determined with a solid-phase assay, the affinity of the receptor fragments for Bgtx would appear to be at most 10-fold lower than what has been observed for the native receptor. This high affinity demonstrates that the α143−210 receptor fragment retains the major structural elements required for Bgtx binding to the native receptor and provides additional strong support for the conclusion from a variety of binding studies that the major determinant for high-affinity Bgtx binding lies within α-subunit residues 173−204 (*9, 10, 62, 63*).

Solid-phase competition assays of ^{125}I-Bgtx binding using cholinergic ligands are also consistent with a considerable nativelike folding of αT68His$_6$. Assays of the αT68His$_6$ fragment using curare, nicotine, and carbamylcholine as competitors yielded IC_{50} values of 110 μM, 200 μM, and 8.5 mM, respectively. These IC_{50} concentrations for competing ligands correspond to K_I values of 58 μM, 105 μM, and 4.5 mM. As expected, the observed affinities are lower than that observed for the native receptor given that only two of the three extracellular domain subsites that have been implicated in the formation of a "multiple-loop" cholinergic ligand binding site are present in our constructs and residues from the adjacent δ- and γ-subunits are absent. The entire extracellular domain of the mouse α1-subunit expressed in mammalian cells and tethered to the membrane by an anchorage sequence failed to show curare-sensitive Bgtx binding (*29*) while bacterially expressed and renatured preparations of the α-subunit ECD from *Torpedo* were reported to have affinities for curare of 0.42 mM (*30*) and 0.2 mM (*31*), respectively. Fusion proteins containing α1-subunit sequences exhibit millimolar IC_{50} values for nicotine competition of Bgtx binding (*10*).

To assess the functionality of the micelle-incorporated preparations, we measured high-affinity ligand binding activity of the αT68M1 receptor fragment in DPC micelles. In a toxin-depletion assay, we measured an IC_{50} value of 30 nM, which is within an order of magnitude of the IC_{50} value (3 nM) obtained with the purified *Torpedo* AChR using this same assay (*64*). This high-affinity Bgtx binding provides evidence that the ECD portion of the micelle-associated αT68M1 fragment is accessible to water-soluble ligands.

A Strategy for NMR Structural Studies of an nAChR Fragment from the ECD. The purified αT68His$_6$ protein at millimolar concentrations self-associates to form large, but soluble aggregates which exhibit a significant overall β-sheet structure as shown by CD analysis. This is consistent with the proposal that aggregation in many proteins is stabilized by intermolecular β-sheet structures (*65*). As shown in CD studies of the αT68His$_6$ protein across a range of protein concentrations, the β-sheet aggregation appears to represent a concentration-dependent process of protein self-association. However, solid-phase competition binding studies which indicate that the monomeric and aggregated forms of the αT68His$_6$ protein exhibit indistinguishable IC_{50} values for Bgtx binding suggest that the folding of the high-affinity Bgtx binding site occurs before the onset of aggregation. A number of proteins involved in β-sheet aggregates have demonstrated nativelike structure and/or properties suggesting that correctly folded proteins (or protein subdomains) then incorrectly self-associate in a manner nondisruptive to their core nativelike structure (*66*).

The αT68His$_6$ protein could be renatured following urea solubilization as a monomer at 20 μM concentrations or below as demonstrated by size-exclusion chromatography. The monomeric αT68His$_6$ protein refolded into a structure with significant β-sheet structure content (∼39%) and a smaller α-helical structure component (∼13%). CD studies of the N-terminal ECD domain of the α-subunit expressed in mammalian cells (*29*) or expressed in *E. coli* and renatured (*30*) suggested that ∼15% of the ECD (∼33 amino acids) is α-helical. These observations are compatible with cryoelectron microscopic studies of the nAChR which reveal an electron density map of the α-subunit ECD that contains three distinct α-helical rods, each extending over at least 12 Å in length (*2*). The 13% α-helical component of the αT68His$_6$mer, which represents ∼9 amino acids, could correspond to a single helix of ∼13 Å (*67*). Our result implies that one of the three putative α-helical rods lies between residues 143 and 210 in the ECD of the α-subunit. This implication is compatible with a recent secondary structure model of the α-subunit ECD that predicts 10 amino acids within residues 130−210 are in an α-helical conformation (*68*).

Homogeneity of the monomeric αT68His$_6$ protein was supported by the highly cooperative, two-state folding transition observed upon incremental urea addition. Nonetheless, at protein concentrations necessary for NMR study, the αT68His$_6$ fragment self-associates to form soluble aggregates despite a rigorous survey of sample conditions (i.e., buffer species, pH, salt content, and cosolvent addition). This behavior was also observed upon concentration of the 1:1 complex formed between Bgtx and monodisperse αT68His$_6$. In seeking a means of dispersing the αT68His$_6$ fragment without disrupting its inherent structure, we turned to lipid and detergent micelles which comprise two-well characterized model membrane systems available for multidimensional solution NMR studies (*50, 69*). We reasoned that membrane-mimicking micelles might disrupt the receptor fragment aggregates by minimizing protein−protein interactions. To anchor the extracellular 68mer portion of the fragment to the micelle surface, we prepared a recombinant αT68M1 fragment containing the M1 transmembrane domain.

In contrast to the αT68His$_6$ protein, the overriding contributor to the formation of a self-associated but soluble αT68M1 protein preparation appeared, somewhat ironically, to be the interaction of the hydrophobic M1 domains. The ability of thrombin protease to completely cleave the receptor fragment from the thioredoxin fusion protein suggested that the receptor sequences were largely accessible. The putative interaction between M1 domains apparently alleviated the receptor fragment self-association that previously occluded 50% of the cleavage sites in the TrxFusSSαT68His$_6$ fusion protein. In addition to greatly facilitating the purification of the αT68M1 fragment, the incorporation of the M1 sequence enabled us to purify the receptor fragment without denaturant and harsh and inefficient refolding procedures.

In CD studies of micelle preparations, we observed a secondary structure transition toward enhanced α-helical content that appeared to saturate at moderate lipid concentrations (up to 10 mM). This suggested that the M1 domain was being inserted into the micelles. In addition, we examined the micelle-incorporated 68mer by dynamic laser light scattering measurements and found evidence for an essentially monodisperse micelle preparation. The molecular weight of the protein-bearing micelles is within the range that is tractable to NMR analysis of isotopically enriched proteins. We postulate that the forces holding the hydrophobic M1 domain in the micelle are generally stronger than the interactions between the M1 domains of the fragments and that the repulsive forces between micelles overwhelm the protein−protein interactions producing in the end a monodisperse suspension. Similar results were obtained for the αT68M1 fragment in SDS micelles. Dynamic laser light scattering measurements indicated that 1 molecule of αT68M1 protein was associated with ∼50 SDS molecules. The uniform solubilization of protein into lipid or detergent micelles for NMR study typically requires very high concentrations of lipid or detergent in order to obtain a very homogeneous population of small micelles that each contain a single polypeptide (*69*). Concentrations 20−100 times the lipid or detergent critical micelle concentrations are typically required for structural studies (*70*).

The Implications of Initial NMR Studies of the Micelle-Associated αT68M1 Fragment. As expected for a relatively large micelle-incorporated protein, the ^{1}H spectrum (data not shown) for the αT68M1 protein in either SDS or DPC micelles is not as highly resolved as a globular protein of comparable molecular weight. Improvement in the line broadening in the ^{1}H and ^{1}H−^{15}N HSQC spectra was used to determine the optimal sample conditions through systematic variation of the lipid or detergent concentration, pH, salt content, and temperature. In addition, several different methods for incorporating the αT68M1 protein into micelles were tested. We are confident that the αT68M1 protein is completely solubilized at a 1000-fold molar excess of SDS as we observed no further change in the HSQC spectrum at higher SDS:protein ratios. In addition, we can clearly discern a large percentage (>75%) of the expected ^{1}H−^{15}N cross-peaks which confirms the presence of stable elements of structure. As anticipated for a large micelle-incorporated protein, the ^{1}H−^{15}N HSQC spectrum is characterized by amide cross-peaks that are broad. A great number of the observed resonances appear to populate a window of proton chemical shifts between 7.7 and 8.6 ppm, a range typically observed for amide protons involved in an α-helical structure (*21*). The broader resonances are centered at 119 ppm (^{15}N) and may correspond to the α-helical residues of the M1 domain embedded in the micelle (*71*).

Our ability to proceed with specific residue assignments will depend on the preparation of αT68M1 protein/micelles containing higher protein concentrations and on the incorporation of both ^{15}N and ^{13}C isotope labels into the αT68M1 protein. These early studies indicate that suitable samples of the αT68M1 fragment at ∼1.5 mM protein concentrations can be prepared. The initial results presented here highlight the great potential for this system in allowing structural studies of the αT68M1 receptor fragment to be pursued by NMR methodologies. An assignment strategy based on initial sequential assignments made through the amide protons of the peptide backbone using three-dimensional ^{1}H−^{15}N NOESY−HSQC (*72*) and ^{1}H−^{15}N TOCSY−HSQC (*73*) experiments will be applied to this system. Additionally, the $^{13}C_\alpha$ and $^{13}C_\beta$ chemical shifts (*74*) and, to a lesser extent, the^{15}N chemical shifts of backbone amide nitrogens (*75*) in proteins are correlated to local secondary structure. An analysis of the deviations of observed chemical shifts from their random coil values may allow for the assignment of residues in α-helical structures within the αT68M1 fragment which can be correlated with α-helical elements of structure observed in cryoelectron microscopic studies of the native nAChR (*15*). The identification of those residues within the αT68M1 protein that either bind to or lie within close proximity to bound cholinergic ligands such as *d*-tubocurarine or nicotine may be possible with future NMR experiments designed to reveal selective chemical shift perturbations.

NMR-based protein structural studies are often hampered with problems of protein aggregation and insolubility. The few strategies for overcoming such problems apart from sample condition manipulations have included removal of insoluble/aggregating domains and sequence re-engineering to increase solubility or to remove unwanted protein−protein interactions (*76*). We propose here that the addition of a terminal hydrophobic domain might serve as a general means of incorporating recombinant protein into lipid or detergent micelles in order to obtain NMR-based structural information that would otherwise be intractable. This approach may be very attractive for proteins or protein fragments that in the native state lie near to or at a membrane surface and which may be stabilized by interactions with polar lipid headgroups.

It is difficult to assess the exact degree to which a protein structure determined in micelles would resemble the native, functional structure. In contrast to the results presented here, few of the previously reported systems for which a micelle approach has been applied have had readily assayable functional properties. It is clear from our analysis that the αT68M1 protein does not become denatured upon micelle incorporation. Furthermore, significant secondary structure is retained as demonstrated by CD analysis. In addition, analysis of the ^{1}H spectrum (data not shown) reveals several well-resolved resonances in the chemical shift region upfield of 0 ppm. Such resonances are lacking in unfolded polypeptides but are characteristic of many structured proteins (*77*). Furthermore, the thermal denaturation CD studies of the micelle-incorporated αT68M1 protein indicate that the αT68M1 fragment retains its protein fold and suggest

structural homogeneity. A significant portion of the secondary structure of the αT68M1 protein remained upon heating to 90 °C. This observation is qualitatively similar to the results obtained upon thermal denaturation of a recombinantly expressed form of the entire mouse α-subunit ECD (*29*).

We have demonstrated that a large, recombinantly produced fragment of the nAChR α-subunit containing crucial elements of the ligand binding domain can be incorporated successfully into detergent or lipid micelles. Two advantages of these micelle environments are the ability to address the problematic aggregation of the $\alpha T68His_6$ receptor fragment and to incorporate the αT68M1 fragment into a membrane-mimicking environment presumably like that found for this region of the α-subunit in the native AChR. The resulting monodisperse receptor fragment preparation is capable of binding Bgtx with high affinity and has features highly conducive to further structural analysis by NMR. The characterization of such a receptor fragment preparation by means of high-resolution, multidimensional NMR spectroscopy would represent an important step toward the elucidation of the structure−function relationship in the ligand-gated ion channel protein superfamily.

ACKNOWLEDGMENT

We thank Dale Mierke (Brown University) and Dusan Uhrin and Paul Barlow (Edinburgh Biomolecular NMR Unit, Edinburgh University) for assistance with the NMR experimentation. Malcolm Walkinshaw (Edinburgh University) kindly provided access to the laser light scattering instrumentation. Additionally, we acknowledge Yingxin Lin and Jennifer Qian Pan for excellent technical assistance.

REFERENCES

1. Karlin, A., and Akabas, M. H. (1995) *Neuron 15*, 1231−1244.
2. Unwin, N. (1993) *J. Mol. Biol. 229*, 1101−1124.
3. Galzi, J.-L., and Changeux, J.-P. (1994) *Curr. Opin. Struct. Biol. 4*, 554−565.
4. Tsigelny, I., Sugiyama, N., Sine, S. M., and Taylor, P. (1997) *Biophys. J. 73*, 52−66.
5. Galzi, J.-L., Revah, F., Black, D., Goeldner, M., Hirth, C., and Changeux, J.-P. (1990) *J. Biol. Chem. 265*, 10430−10437.
6. Galzi, J.-L., Bertrand, D., Devillers-Thiery, A., Revah, F., Bertrand, S., and Changeux, J.-P. (1991) *FEBS Lett. 294*, 198−202.
7. Wilson, P. T., Gershoni, J. M., Hawrot, E., and Lentz, T. L. (1984) *Proc. Natl. Acad. Sci. U.S.A. 81*, 2553−2557.
8. Wilson, P. T., Hawrot, E., and Lentz, T. L. (1988) *Mol. Pharmacol. 34*, 643−651.
9. Fuchs, S., Barchan, D., Kachalsky, S., Neumann, D., Aladjem, M., Vogel, Z., Ovadia, M., and Kochva, E. (1993) *Ann. N.Y. Acad. Sci. 681*, 126−139.
10. Chaturvedi, V., Donnelly-Roberts, D. L., and Lentz, T. L. (1993) *Biochemistry 32*, 9570−9576.
11. Chiara, D. C., and Cohen, J. B. (1997) *J. Biol. Chem. 272*, 32940−32950.
12. Martin, M., Czajkowski, C., and Karlin, A. (1996) *J. Biol. Chem. 271*, 13497−13503.
13. Sine, S. M. (1993) *Proc. Natl. Acad. Sci. 90*, 9436−9440.
14. Sine, S. M., Kreienkamp, H.-J., Bren, N., Maeda, R., and Taylor, P. (1995) *Neuron 15*, 205−211.
15. Unwin, N. (1995) *Nature 373*, 37−43.
16. Unwin, N. (1996) *J. Mol. Biol. 257*, 586−596.
17. Basus, V. J., Song, G., and Hawrot, E. (1993) *Biochemistry 32*, 12290−12298.
18. Williams, G., Ruegg, N., Birch, A., Weber, C., Hofstadter, K., Robinson, J. A., Aguet, M., Garotta, G., Schlatter, D., and Huber, W. (1995) *Biochemistry 34*, 1787−1797.
19. Overduin, M., Tong, K. I., Kay, C. M., and Ikura, M. (1996) *J. Biomol. NMR 7*, 173−189.
20. Fushman, D., Najmabadi-Haske, T., Cahill, S., Zheng, J., LeVine, H., and Cowburn, D. (1998) *J. Biol. Chem. 273*, 2835−2843.
21. Opella, S. J., Marassi, F. M., Gesell, J. J., Valente, A. P., Kim, Y., Oblatt-Montal, M., and Montal, M. (1999) *Nat. Struct. Biol. 6*, 374−379.
22. van de Ven, F. J. M., van Os, J. W. M., Aelen, J. M. A., Wymenga, S. S., Remerowski, M. L., Konings, R. N. H., and Hilbers, C. W. (1993) *Biochemistry 32*, 8322−8328.
23. Williams, K. A., Farrow, N. A., Deber, C. M., and Kay, L. E. (1996) *Biochemistry 35*, 5145−5157.
24. Almeida, F. C. L., and Opella, S. J. (1997) *J. Mol. Biol. 270*, 481−495.
25. Pervushin, K. V., Orekhov, V. Y., Popov, A. I., Musina, L. Y., and Arseniev, A. S. (1994) *Eur. J. Biochem. 219*, 571−583.
26. MacKenzie, K. R., Prestegard, J. H., and Engleman, D. M. (1997) *Science 276*, 131−133.
27. Gershoni, J. M. (1987) *Proc. Natl. Acad. Sci. U.S.A. 84*, 4318−4321.
28. Aronheim, A., Eshel, Y., Mosckovitz, R., and Gershoni, J. M. (1988) *J. Biol. Chem. 263*, 9933−9937.
29. West, A. P., Bjorkman, P. J., Dougherty, D. A., and Lester, H. A. (1997) *J. Biol. Chem. 41*, 25468−25473.
30. Schrattenholz, A., Pfeiffer, S., Pejovic, V., Rudolph, R., Godovac-Zimmermann, J., and Maelicke, A. (1998) *J. Biol. Chem. 273*, 32393−32399.
31. Alexeev, T., Krivoshein, A., Shevalier, A., Kudelina, I., Telyakova, O., Vincent, A., Utkin, Y., Hucho, F., and Tsetlin, V. (1999) *Eur. J. Biochem. 259*, 310−319.
32. Sambrook, J., Fritsch, E. F., and Maniatis, T. (1989) *Molecular Cloning: A Laboratory Manual*, 2nd ed., Cold Spring Harbor Laboratory, Cold Spring Harbor, NY.
33. Lowry, O. H., Rodebrough, N. J., Farr, A. L., and Randall, R. J. (1951) *J. Biol. Chem. 193*, 265−275.
34. Laemmli, U. K. (1970) *Nature 227*, 680−685.
35. Schagger, H., and von Jagow, G. (1987) *Anal. Biochem. 166*, 368−379.
36. Fulachier, M.-H., Mourier, G., Cotton, J., Servent, D., and Menez, A. (1994) *FEBS Lett. 338*, 331−338.
37. Czajkowski, C., DiPaolo, M., Bodkin, M., Salazar-Jimenez, G., Holtzman, E., and Karlin, A. (1989) *Arch. Biochem. Biophys. 272*, 412−420.
38. Schmidt, J., and Raftery, M. A. (1974) *J. Neurochem. 23*, 617−623.
39. Rosenthal, J. A., Hsu, S. H., Schneider, D., Gentile, L. N., Messier, N. J., Vaslet, C. A., and Hawrot, E. (1994) *J. Biol. Chem. 269*, 11178−11185.
40. Pearce, S. F. A., Preston-Hurlburt, P., and Hawrot, E. (1990) *Proc. R. Soc. London B 241*, 207−213.
41. Perczel, A., Park, K., and Fasman, G. D. (1992) *Anal. Biochem. 203*, 83−93.
42. Killian, J. A., Trouard, T. P., Greathouse, D. V., Chupin, V., and Lindblom, G. (1994) *FEBS Lett. 348*, 161−165.
43. Marion, D., Ikura, M., Tschudin, R., and Bax, A. (1989) *J. Magn. Reson. 85*, 393−399.
44. Kay, L. E., Keifer, P., and Saarinen, T. (1992) *J. Am. Chem. Soc. 114*, 10663−10665.
45. Shaka, A. J., Barker, P. B., and Freeman, R. (1985) *J. Magn. Reson. 64*, 547−552.
46. Piotto, M., Saudek, V., and Sklenar, V. (1992) *J. Biomol. NMR 2*, 661−666.
47. Mehta, D. V., DiGate, R. J., Banville, D. L., and Guiles, R. D. (1997) *Protein Expression Purif. 11*, 86−94.
48. Sine, S. M., Quiram, P., Papanikolaou, F., Kreienkamp, H.-J., and Taylor, P. (1994) *J. Biol. Chem. 269*, 8808−8816.
49. Cheng, Y. C., and Prusoff, W. (1973) *Biochem. Pharmacol. 22*, 3099−3108.
50. Opella, S. J. (1997) *Nat. Struct. Biol. 4*, 845−848.

51. Chupin, V., Killian, J. A., Breg, J., de Jongh, H. H. J., Boelens, R., Kaptein, R., and de Kruijff, B. (1995) *Biochemistry 34*, 11617−11624.
52. Johnson, W. C. (1990) *Proteins: Struct., Funct., Genet. 7*, 205−214.
53. Henry, G. D., and Sykes, B. D. (1994) *Methods Enzymol. 239*, 515−535.
54. Lauterwein, J., Bosch, C., Brown, L. R., and Wuthrich, K. (1979) *Biochim. Biophys. Acta 556*, 244−264.
55. McIntosh, L. P., and Dahlquist, F. W. (1990) *Q. Rev. Biophys. 23*, 1−38.
56. Barchan, D., Kachalsky, S., Neumann, D., Vogel, Z., Ovidia, M., Kochva, E., and Fuchs, S. (1992) *Proc. Natl. Acad. Sci. U.S.A. 89*, 7717−7721.
57. Fraenkel, Y., Navon, G., Aronheim, A., and Gershoni, J. (1990) *Biochemistry 29*, 2617−2622.
58. Conti-Tronconi, B. M., McLane, K. E., Raftery, M. A., Grando, S. A., and Protti, M. P. (1994) *Crit. Rev. Biochem. Mol. Biol. 29*, 69−123.
59. Sine, S. M. (1997) *J. Biol. Chem. 272*, 23521−23527.
60. Weber, M., and Changeux, J.-P. (1974) *Mol. Pharmacol. 10*, 1−14.
61. Sine, S. M., and Claudio, T. (1991) *J. Biol. Chem. 266*, 13679−13689.
62. Gershoni, J. M., Hawrot, E., and Lentz, T. L. (1983) *Proc. Natl. Acad. Sci. U.S.A. 80*, 4973−4977.
63. Wilson, P. T., Lentz, T. L., and Hawrot, E. (1985) *Proc. Natl. Acad. Sci. U.S.A. 82*, 8790−8794.
64. Wilson, P. T., and Lentz, T. L. (1988) *Biochemistry 27*, 6667−6674.
65. Speed, M. A., Wang, D. I. C., and King, J. (1996) *Nat. Biotechnol. 14*, 1283−1287.
66. Oberg, K., Chrunyk, B. A., Wetzel, R., and Fink, A. L. (1994) *Biochemistry 33*, 2628−2634.
67. Brandon, C., and Tooze, J. (1991) *Introduction to Protein Structure*, Garland Publishing, Inc., New York.
68. Ortells, M. O. (1997) *Proteins: Struct., Funct., Genet. 29*, 391−398.
69. Opella, S. J., Kim, Y., and McDonnell, P. (1994) *Methods Enzymol. 239*, 536−560.
70. McDonnell, P. A., and Opella, S. J. (1993) *J. Magn. Reson. B 102*, 120−125.
71. Cornilescu, G., Delaglio, F., and Bax, A. (1999) *J. Biomol. NMR 13*, 289−302.
72. Marion, D., Kay, L. E., Sparks, S. W., Torchia, S. W., and Bax, A. (1989) *J. Am. Chem. Soc. 111*, 1515−1517.
73. Marion, D., Driscoll, P. C., Kay, L. E., Wingfield, P. T., Bax, A., Gronenborn, A. M., and Clore, G. M. (1989) *Biochemistry 28*, 6150−6156.
74. Wishart, D. S., and Sykes, B. D. (1994) *Methods Enzymol. 239*, 363−392.
75. Bax, A., and Grzesiek, S. (1993) in *NMR of Proteins* (Clore, G. M., & Gronenborn, A. M., Eds.) pp 33−52, CRC Press, Inc., Boca Raton, FL.
76. Chen, J., Skehel, J. J., and Wiley, D. C. (1998) *Biochemistry 37*, 13643−13649.
77. Cavanagh, J., Fairbrother, W. J., Palmer, A. G., and Skelton, N. J. (1996) *Protein NMR Spectroscopy: Principles and Practice*, Academic Press, Inc., San Diego, CA.

BI983007Q